IOPscience iopscience.iop.org

Home Search Collections Journals About Contact us My IOPscience

The effect of threading dislocations on optical absorption and electron scattering in strongly mismatched heteroepitaxial III–V compound semiconductors on silicon

This article has been downloaded from IOPscience. Please scroll down to see the full text article.

2002 J. Phys.: Condens. Matter 14 13195

(http://iopscience.iop.org/0953-8984/14/48/368)

View the table of contents for this issue, or go to the journal homepage for more

Download details:
IP Address: 171.66.16.97
The article was downloaded on 18/05/2010 at 19:16

Please note that terms and conditions apply.

INSTITUTE OF PHYSICS PUBLISHING JOURNAL OF PHYSICS: CONDENSED MATTER

J. Phys.: Condens. Matter **14** (2002) 13195–13201 PII: S0953-8984(02)54017-0

The effect of threading dislocations on optical absorption and electron scattering in strongly mismatched heteroepitaxial III–V compound semiconductors on silicon

Erwin Peiner, Andreas Guttzeit and Hergo-Heiurich Wehmann

Institut für Halbleitertechnik, Technische Universität Braunschweig, Hans-Sommer-Str. 66, D-38106 Braunschweig, Germany

E-mail: e.peiner@tu-bs.de

Received 27 September 2002
Published 22 November 2002
Online at stacks.iop.org/JPhysCM/14/13195

Abstract
The effect of threading dislocations on the optical and electrical properties of InP and GaAs heteroepitaxial layers on (001) silicon was investigated. Charged deep states act as scattering centres for electrons, thus affecting the electron mobility at low temperatures. The electric field arising from charged dislocations causes enhanced optical absorption at wavelengths near the fundamental absorption edge. The mean charge of the threading dislocations in GaAs/Si was found to be considerably higher than that for InP/Si. A model is described relating this effect to a regular arrangement of α-type 60° dislocations at extended twin defects which were observed in InP/Si but were absent in GaAs/Si.

1. Introduction

Integration of high-performance III–V compound semiconductor optoelectronic devices with silicon is of sustained interest in relation to high-speed optical data transmission from chip to chip and from board to board or combining the superior radiation resistance of InP with the strength and cost effectiveness of silicon, e.g. for solar cells [1–3]. Direct heteroepitaxy of III–V compounds on silicon with delayed metallization may be ultimately preferable to bonding techniques, since it can easily scale with the shrinking dimensions and power limits of silicon ICs. An important advantage is the typically very low resistance across the heteroepitaxial interface [4]. Feasibility of heteroepitaxy for optoelectronic transmitters and receivers was demonstrated using pre-processed circuitry without thermal damage [2].

The life to failure of an optoelectronic transmitter, as the device being most susceptible to degradation, is related to stress and lattice defects in the heteroepitaxial layers arising from the

 © 2002 IOP Publishing Ltd Printed in the UK

mismatch between layer and substrate in both the lattice parameters and the thermal expansion coefficients. The cross-sectional TEM photographs in figure 1 show the arrangement of defects in an InP layer on silicon comprising a nucleation layer and a thick functional layer on top:

- At the layer–substrate interface a grid of misfit dislocations is generated during the early stages of growth, relieving the strain due to lattice mismatch. During the coalescence of nucleation islands, stacking faults and microtwins are generated.
- Dislocations are bent upwards from the interface towards the surface. Threading dislocation density decreases with increasing layer thickness due to dislocation reactions (e.g. annihilation) at elevated temperatures where dislocations are mobile. In figure 2 the threading dislocation density N_{dis} is displayed versus layer thickness. The straight line corresponds to a model calculation for InP/Si after [6]. Dislocation etching was used to determine N_{dis}. Typical etch pit patterns obtained by SEM are shown as insets in figure 2.
- As a specific feature in InP/Si, large twin defects (lamellae of thickness several tens of nanometres) are observed (figure 1 and [5]). These defects are extended in the $[1\bar{1}0]$ crystal direction, acting as traps for dislocations. This can be concluded from the regular arrangement of the dislocations in thick InP/Si layers as shown in the upper right inset of figure 2. In cases where such etch pit patterns are observed, the measured dislocation density is much higher than expected according to the Dodson model. Good agreement with the model is found for thin layers and as well for thick layers if twin lamellae are scarcely observed. Very low densities of twin lamellae are obtained by selective epitaxy (filled circles) and by a sophisticated process (filled squares) comprising three epitaxy techniques [7–9].

In this contribution the results of various investigations are described in order to support the distribution of extended defects in highly mismatched InP/Si and GaAs/Si suggested by TEM and dislocation etching. In detail we studied:

- lattice strain by temperature-dependent photoreflectance (PR) spectroscopy,
- deep states at the dislocation core by low-temperature photoluminescence (PL) spectroscopy,
- electric fields arising from dislocations by optical absorption spectroscopy and
- the charging state of the dislocation core by temperature-dependent van der Pauw/Hall measurements.

2. Experimental details

Epitaxial InP and GaAs layers were grown on exactly [001]-oriented silicon wafers by metal–organic vapour-phase epitaxy (MOVPE). We started with a thin nucleation layer (15–40 nm) deposited at 400 °C. Subsequently, a thick functional layer ($h \approx 2\ \mu$m) was grown on top of the nucleation layer at 640 and 700°C for InP and GaAs, respectively. For more details on the growth process, see [5].

Optical characterization of the layers was performed using PR, PL and spectroscopic ellipsometry (SE) in the spectral range around the band-gap-equivalent wavelength. By means of PR, the laser-induced modulation of the dielectric function was measured; it exhibits distinct features at the critical points of the band structure [10]. Radiative recombination of electron–hole pairs via deep states was investigated by means of PL. By SE, changes in amplitude and phase of elliptically polarized radiation upon reflection at the epilayer were measured. The absorption coefficient $\bar{\alpha}$ and the index of refraction were determined on the basis of a parametrized three-layer model comprising the silicon substrate, the epitaxial layer and a native

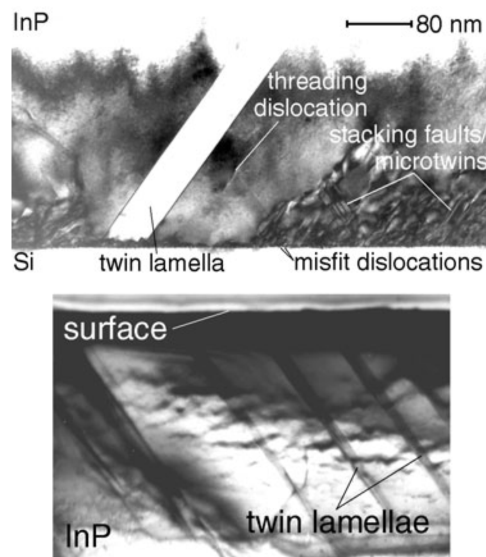

Figure 1. Cross-sectional TEM photographs of InP on silicon showing the typical arrangement of extended defects in this highly mismatched system.

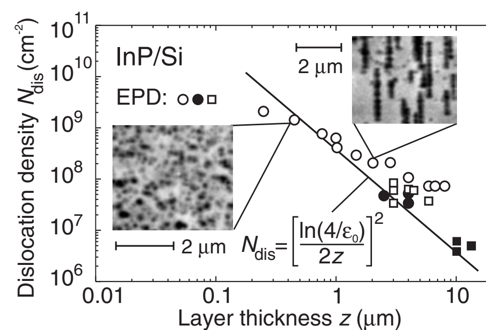

Figure 2. Density of threading dislocations in InP/Si versus layer thickness. Data points represented by the open and filled squares are taken from [7–9].

oxide layer on top [11]. Electron concentration and mobility were determined by the stripping van der Pauw technique [12]. For differential analysis of thin sublayers, each measurement cycle was followed by defined thinning of the layer.

3. Results

3.1. Strain

Figure 3 shows PR spectra of an InP/Si heteroepitaxial layer and an InP/InP homoepitaxial reference layer measured in the temperature range between 12 and 296 K. At low temperatures, resonances related to critical points of the valence band structure are visible, which are assigned to transitions from the light/heavy hole (E_g^{V1}) and split-off valence bands (E_g^{V3}) into the conduction band. Towards room temperature, the split-off band resonance has Franz–Keldysh

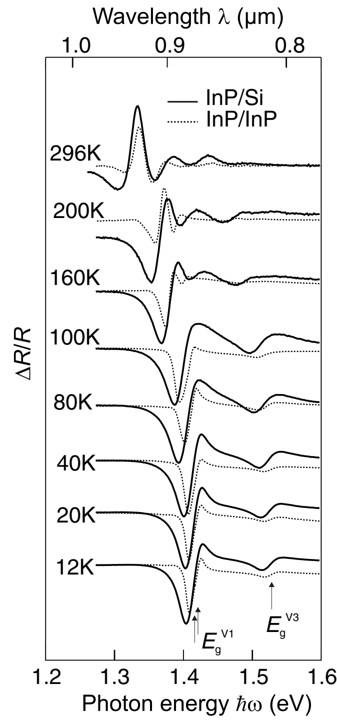

Figure 3. Temperature-dependent PR spectra of InP/Si in comparison with an InP/InP reference.

oscillations superimposed on it. Tensile strain was generated in InP/Si during cooling down from growth temperature owing to the different thermal expansion coefficients of the layer and the substrate. This leads to the observed energy shift between the InP/Si and InP/InP features. We find a shift of around 7 meV independent of temperature, which is very low with respect to that for GaAs/Si [10].

3.2. Deep levels

Defect levels in the band gap are expected at dislocations, e.g. in the core of 60° dislocations, owing to the lack of binding partners of the atoms for saturating their chemical bonds [13]. In figure 4, PL spectra are displayed which were measured at 11 K with InP/Si of different dislocation densities. In addition to the band–band recombination peak at 1.4 eV, a broad emission band is observed at 1.15 eV. The intensity ratio between the deep-level and band–band emissions increases with the dislocation density. Thus, we attribute the deep-level emission to dislocation-related transitions, e.g. via deep levels located at the dislocation core. Such transitions may be supported by the band bending around the dislocation.

We consider the occupation of the deep levels which are periodically localized along the dislocation line, assuming that the dangling bonds at the imperfection centres are of the same nature. If all traps are filled with electrons, we find an excess charge at the dislocation core. In III–V compounds the charge ζ (in units of the elementary charge) added per possible site is different for α-type and β-type dislocations: $\zeta_\alpha = 0.17$ and $\zeta_\beta = 0.83$ [14]. Thus, for layers comprising both types of dislocation at densities of N_α and N_β, we may define a mean

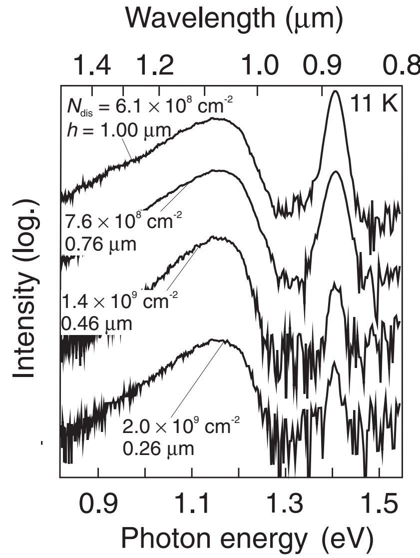

Figure 4. Dislocation-related low-temperature PL of InP/Si; the numbers given represent InP layer thickness h and threading dislocation density N_{dis}.

dislocation charge:

$$\zeta_{\mathrm{dis}} = \frac{\zeta_\alpha + \zeta_\beta \frac{N_\beta}{N_\alpha}}{1 + \frac{N_\beta}{N_\alpha}}; \qquad (1)$$

i.e. at $N_\beta \ll N_\alpha$ we find $\zeta_{\mathrm{dis}} = \zeta_\alpha = 0.17$ and at $N_\beta = N_\alpha$ we obtain $\zeta_{\mathrm{dis}} = 0.5$.

3.3. Optical absorption

Bulk direct band-gap semiconductors are transparent in the wavelength range above the band-gap-equivalent wavelength. However, localized electric fields arising from point defects or dislocations cause increased absorption in this range [11]. Figure 5 shows the spectral dependence of the absorption coefficient of thin InP and GaAs nucleation layers measured by SE. The solid curves were calculated on the basis of the microfield model of absorption [11]. At large dislocation density the curves approach straight lines with slopes proportional to $1/(\zeta_{\mathrm{dis}}\sqrt{N_{\mathrm{dis}}})$. Quantitative analysis yields a ratio of $\zeta_{\mathrm{dis}}^{\mathrm{InP}}/\zeta_{\mathrm{dis}}^{\mathrm{GaAs}} = 0.43$ of the mean dislocation charges in InP and GaAs, respectively. Assuming that most of the threading dislocations in InP/Si are trapped at twin lamellae, these dislocations can be expected to be of identical types. Considering the derived much lower mean dislocation charge in InP/Si versus GaAs/Si and equation (1), we deduce that α-dislocations are predominant in InP/Si. Both α-type and β-type dislocations are expected to occur in GaAs, which has a stacking fault energy five times higher. Correspondingly, extended twin defects were not observed in GaAs/Si.

3.4. Electron scattering

Electron transport is affected by scattering at charged dislocations. The resulting electron mobility in InP/Si and GaAs/Si can thus be considered as a superposition of the intrinsic mobility of the bulk material and a contribution due to the charged threading dislocations. The

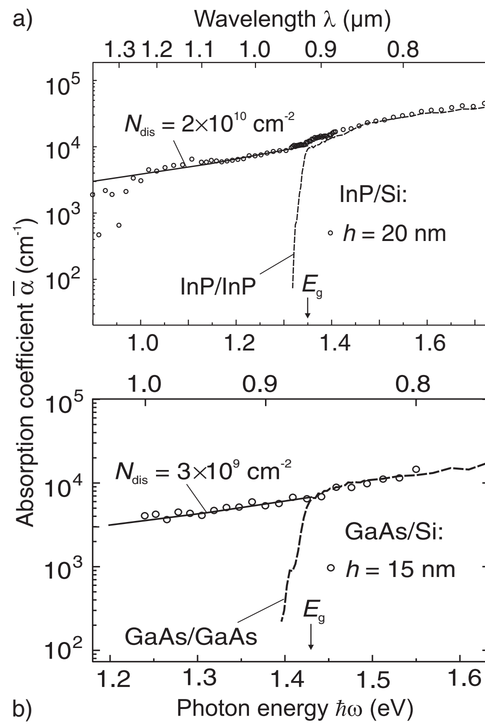

Figure 5. Optical absorption of thin InP (a) and GaAs (b) layers on silicon in the spectral range above the band-gap-equivalent wavelength.

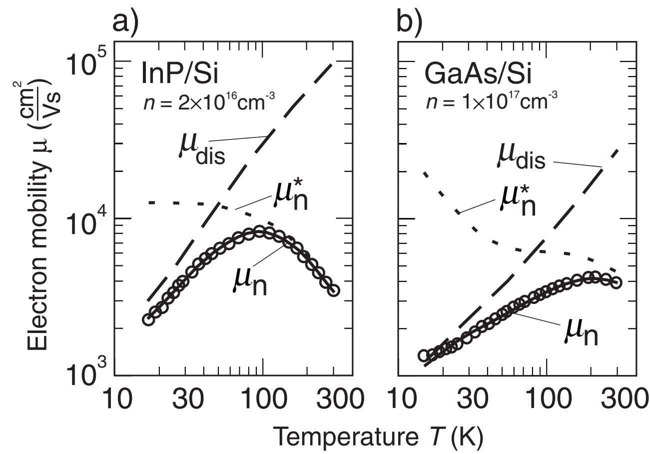

Figure 6. The effect of dislocations on the temperature dependence of the electron mobility in InP (a) and GaAs (b) on silicon; the electron concentrations n are 2×10^{16} and 1×10^{17} cm^{-3}, respectively.

latter is proportional to $1/(\zeta_{dis}^2 N_{dis})$. In figure 6 the temperature dependences of the mobilities of thin sublayers of InP/Si and GaAs/Si samples are shown. The dislocation densities are $(2.0 \pm 0.5)\times 10^8$ cm^{-2} and $(7 \pm 2)\times 10^8$ cm^{-2} for InP/Si and GaAs/Si, respectively.

The solid curves in figure 6 are calculated considering the overall electron mobility as a superposition of the intrinsic mobility of the bulk material and a contribution due to the charged threading dislocations according to Matthiessen's rule [12]. Using the mean dislocation charge as a fitting parameter, we found $\zeta_{dis} = 0.11 \pm 0.03$ for InP and $\zeta_{dis} = 0.5 \pm 0.2$ for GaAs. According to equation (1), we can conclude that α-dislocations are the predominant dislocation type in InP/Si, i.e. $N_\beta \ll N_\alpha$. For GaAs/Si we obtain $N_\beta = N_\alpha$, i.e. equal densities of the two dislocation types. This is in accordance with the results of the optical absorption measurements and supports the trapping of dislocations at twin lamellae in InP/Si.

4. Conclusions

The distribution of extended defects in highly mismatched InP and GaAs on silicon was addressed. A model was described and verified by optical and electrical measurements, showing different behaviour of InP and GaAs. In InP/Si, α-type threading dislocations which are trapped at twin lamellae are predominant, while both α-type and β-type dislocations are effective in GaAs/Si. Further improvement of the quality of InP/Si for optoelectronic device applications requires that extended twin defects are suppressed. This may be accomplished by optimizing the two-dimensional growth of the nucleation layer, e.g. by starting the process with GaAs [5].

References

[1] Taylor P J, Jesser W A, Benson J D, Martinka M, Dinan J H, Bradshaw J, Lara-Taysing M, Leavitt R P, Simonis G, Chang W, Clark W W III and Bertness K A 2001 Optoelectronic device performance on reduced threading dislocation density GaAs/Si *J. Appl. Phys.* **89** 4365–75

[2] Fehly D, Schlachetzki A, Bakin A S, Guttzeit A and Wehmann H-H 2001 Monolithic InGaAsP optoelectronic devices with silicon electronics *IEEE J. Quantum Electron.* **37** 1246–52

[3] Walters R J, Romero M J, Araújo D, García R, Messenger S R and Summers G P 1999 Detailed defect study in proton irradiated InP/Si solar cells *J. Appl. Phys.* **86** 3584–9

[4] Bartels A, Peiner E and Schlachetzki A 1995 Substrate effect on the transport properties of semiconducting films *J. Appl. Phys.* **77** 1621–6

[5] Peiner E, Wehmann H-H, Iber H, Mo S, Tang G-P, Bartels A, Schlachetzki A, Koch A, Dettmer K and Hollfelder M 1997 High-quality $In_{0.53}Ga_{0.47}As$ on exactly (001)-oriented Si grown by metal–organic vapour-phase epitaxy *J. Cryst. Growth* **172** 44–52

[6] Dodson B W 1991 Stress accommodation in large-mismatch systems *J. Cryst. Growth* **111** 376–82

[7] Sugo M, Takanashi Y, Al-jassim M M and Yamaguchi M 1990 Heteroepitaxial growth and characterization of InP on Si substrates *J. Appl. Phys.* **68** 540–7

[8] Tachikawa M, Yamada T, Sasaki T, Mori H and Kadota Y 1995 Laser-diode-quality InP/Si grown by hydride vapour phase epitaxy *Japan. J. Appl. Phys.* **34** L657–9

[9] Yamada T, Tachikawa M, Sasaki T, Mori H and Kadota Y 1997 7000 h continuous wave operation of multiple quantum well laser on Si at 50 °C *Appl. Phys. Lett.* **70** 1614–15

[10] Kuz'menko R V, Gansha A V, Bochurova O V, Domashevskaya É P, Schreiber J, Hildebrandt S, Mo S, Peiner E and Schlachetzki A 2000 Temperature dependence of residual stress in epitaxial GaAs/Si(100) films determined from photoreflectance spectroscopy data *Semiconductors* **34** 73–80

[11] Iber H, Peiner E and Schlachetzki A 1996 The effect of dislocations on the optical absorption of heteroepitaxial InP and GaAs on Si *J. Appl. Phys.* **79** 9273–7

[12] Bartels A, Peiner E and Schlachetzki A 1995 The effect of dislocations on the transport properties of InP/Si *J. Appl. Phys.* **78** 6141–6

[13] Alexander H and Teichler H 1996 Dislocations in materials science and technology *Electronic Structure and Properties of Semiconductors* vol 4, ed R W Cahn, P Haasen, E J Kramer and W Schröter (Weinheim: VCH) pp 249–319

[14] Masut R, Penchina C M and Farvacque J L 1982 Occupation statistics of dislocation deep levels in III–V compounds *J. Appl. Phys.* **53** 4964–9